Electronic Supplementary Material (ESI) for Environmental Science: Nano.

Supplementary Data

Microwave-assisted synthesis of Z-scheme heterojunction Ag/AgBr@BiOBr/Bi_2O_3 photocatalyst for efficient organic pollutants degradation under visible light

Van Quang Nguyen,[a,b,1] Manjiri A. Mahadadalkar,[a] Abdelrahman M.Rabie,[a,c,1] and Jae-Jin Shim[a,*]

[a]*School of Chemical Engineering, Yeungnam University, 280 Daehak-ro, Gyeongsan, Gyeongbuk 38541, Republic of Korea.*

[b]*Faculty of Road and Bridge Engineering, The University of Da Nang – University of Science and Technology, 54 Nguyen Luong Bang, Da Nang 550000, Vietnam.*

[c]*Petrochemicals Department, Egyptian Petroleum Research Institute, Cairo 11727, Egypt.*

[1] These authors contributed equally to this work.

*Corresponding author. Email address: jjshim@yu.ac.kr (J.-J. Shim).

S1. Synthesis of pure BiOBr sample

The BiOBr sample was synthesized by a hydrothermal method. Typically, 0.36 g of KBr was dissolved in 20 ml of DI water. Subsequently, 0.97 g of $Bi(NO_3)_3{\cdot}5H_2O$ was added to the KBr solution. The mixture was stirred for 30 min before transferring to a 30 ml-stainless autoclave. The reaction was conducted at 160 °C for 12 h. The white solid obtained after the reaction was collected and washed several times with DI water to remove the chemical residues. Finally, the sample was dried overnight in an oven at 60 °C. **Fig. S1a** presents the XRD patterns of BiOBr.

S2. Synthesis and characterization of the pure Bi_2O_3 sample

Typically, 0.075 g of CTAB was completely dissolved in 50 ml of DI water, followed by the addition of 1 ml of 70% HNO_3. Then, 1.063 g of $Bi(NO_3)_3 \cdot 5H_2O$ was added to the above solution. The reaction was carried out at room temperature for 3 h. A white solid was collected by filtration and washed with DI water until it reached pH = 7. Finally, the sample was dried in an oven at 60 °C for 12 h. The XRD pattern of the Bi_2O_3 sample is shown in **Fig. S1b**.

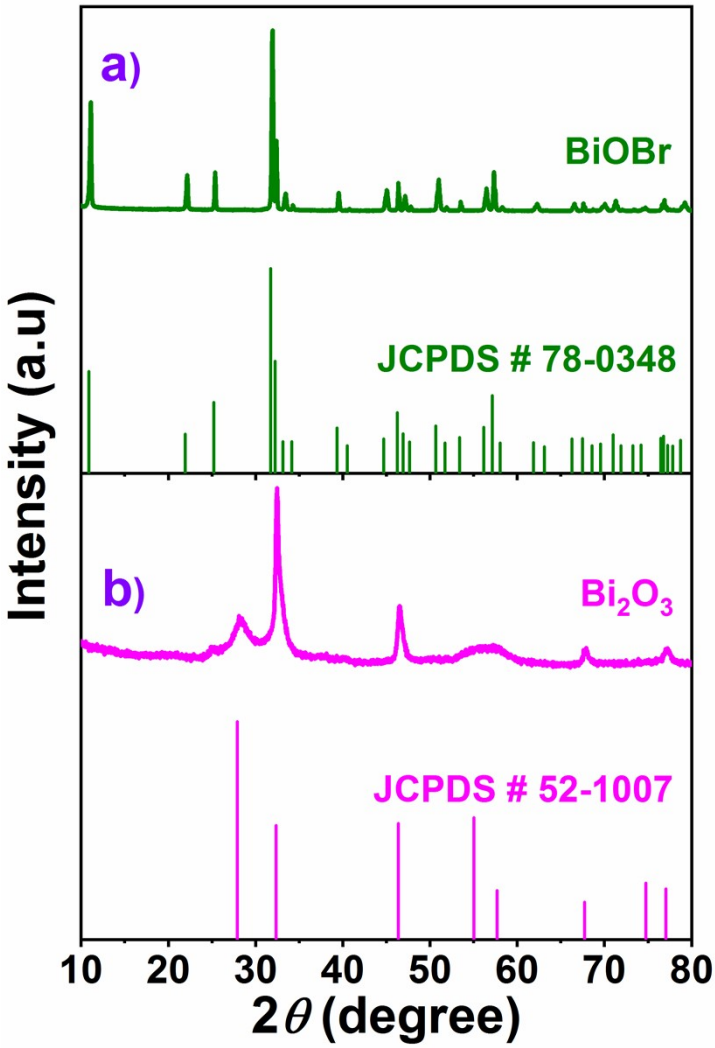

Fig. S1. XRD patterns of pure BiOBr (a) and Bi_2O_3 (b) samples.

S3. Characterization of the as-prepared catalysts

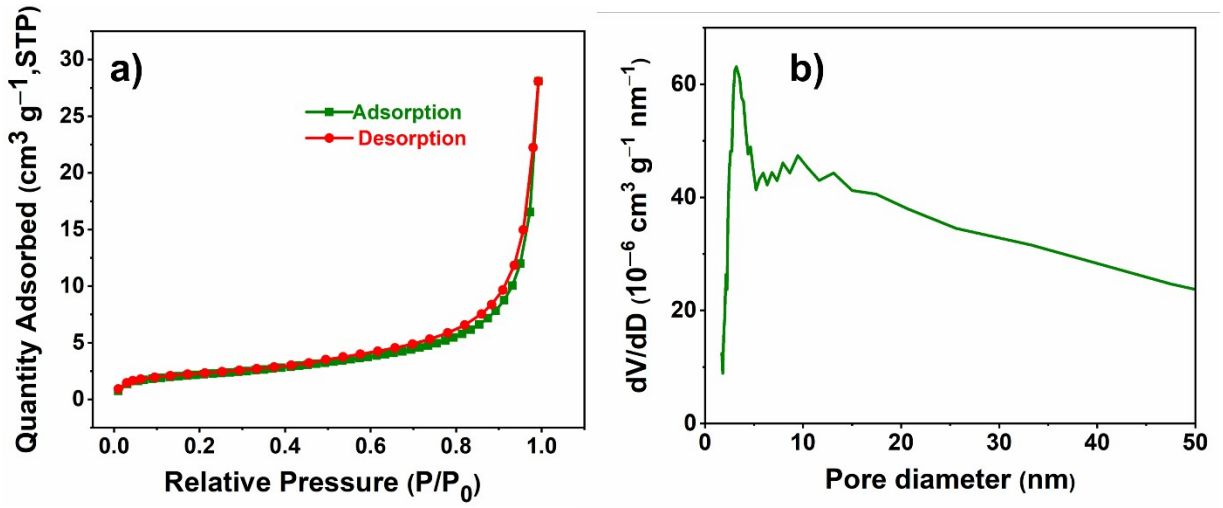

Fig. S2. (a) Nitrogen adsorption-desorption isotherm and (b) pore-size distribution of the as-prepared Ag/AgBr@BiOBr/Bi_2O_3catalyst.

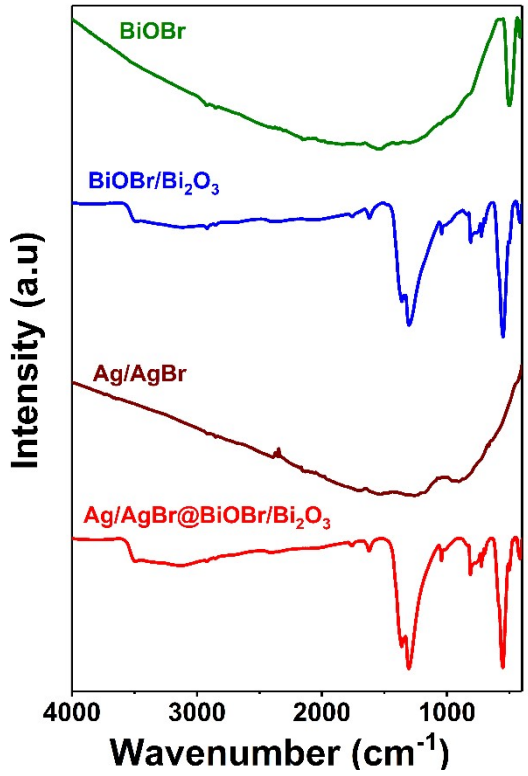

Fig. S3. FTIR spectra of the prepared materials.

S4. Calculation of conduction band (CB) and valence band (VB):

The bandgaps estimated from Tauc plots were 2.72, 2.80, and 2.34 eV for BiOBr, Bi_2O_3, and AgBr, respectively. The CB and VB edge positions (E_{CB} and E_{VB}, respectively) of semiconductors can be calculated using the following empirical formula [1, 2, 3]:

$$E_{CB} = \chi - E_e - 0.5E_g \quad \textbf{(Eq. S1)}$$

$$E_{VB} = E_{CB} + E_g \quad \textbf{(Eq. S2)}$$

where the χ represents the electronegativity of the semiconductor, which is the geometric mean of the electronegativity of the constituent atoms and is about 6.17 [4], 6.24 [1], and 4.42 eV [2] for BiOBr, Bi_2O_3, and AgBr, respectively; E_e is the energy of free electrons on the hydrogen scale (4.5 eV vs. NHE); and E_g is the energy of bandgap. Using Eqs. **S1** and **S2**, E_{CB} was obtained as +0.31, +0.34, and −1.25 eV and E_{VB}, as +3.03, +3.14, and +1.09 eV for BiOBr, Bi_2O_3, and AgBr, respectively. The values are similar to the literature [1, 2, 3].

S5. Comparison of photodegradation performances of the as-prepared catalysts

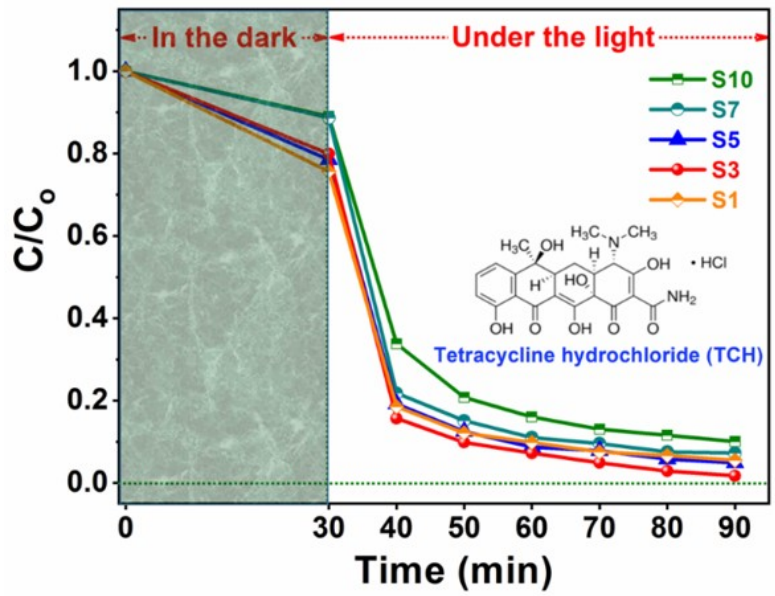

Fig. S4. Photodegradation of a 10 mg L^{-1} aqueous solution of TCH on the Ag/AgBr@BiOBr/Bi_2O_3 catalysts (S1, S3, S5, S7, and S10, synthesized using 100, 300, 500, 700, and 1000 μl of 0.1 M $AgNO_3$ solution, respectively). Photodegradation conditions: catalyst loading of 0.5 g L^{-1}, 10 mg L^{-1} of TCH, and 150 W Xe lamp-solar simulator.

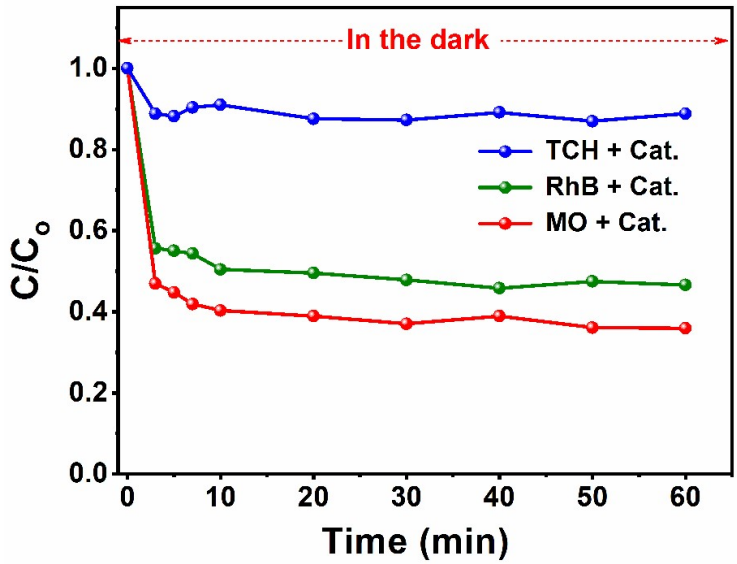

Fig. S5. Adsorption kinetics of Ag/AgBr@BiOBr/Bi_2O_3 sample with three different pollutants in the dark (Catalyst loading of 0.3 g L^{-1}, initial pollutant concentrations of 10 mg L^{-1}).

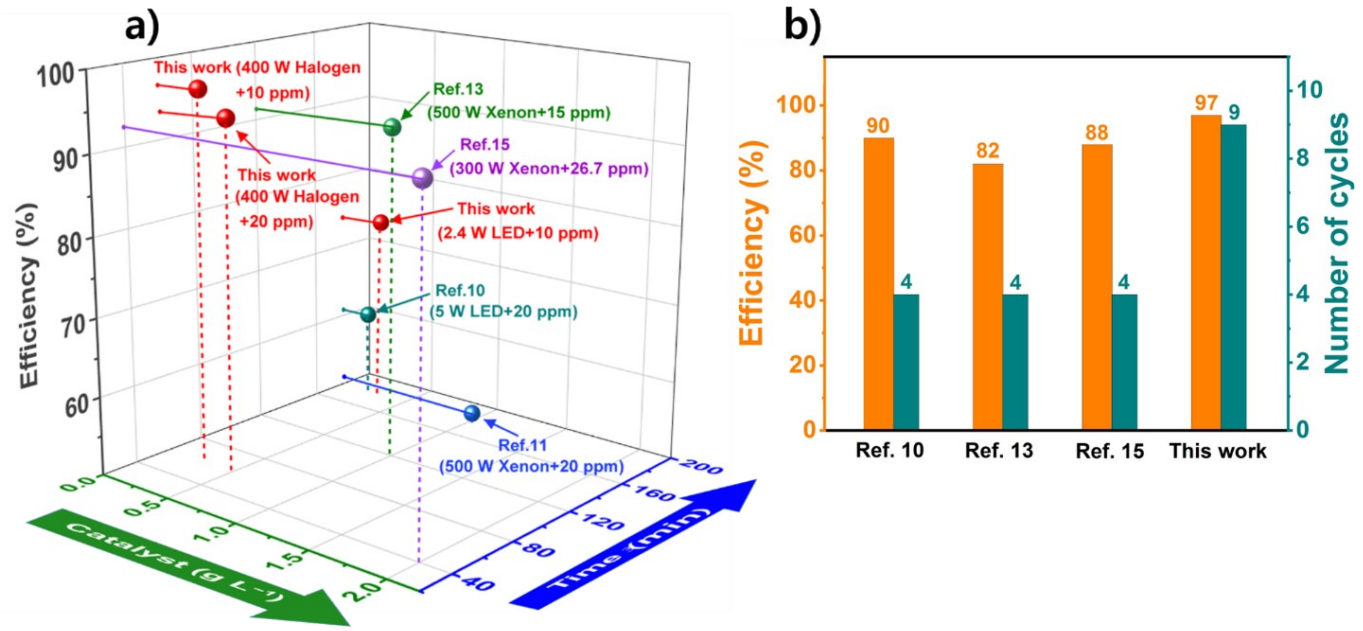

Fig. S6. Comparison of the photocatalytic performance (a) and reusability (degradation efficiency after reuse cycles) (b) in the MO degradation of Ag- and Bi-containing photocatalysts reported in the literature and this work.

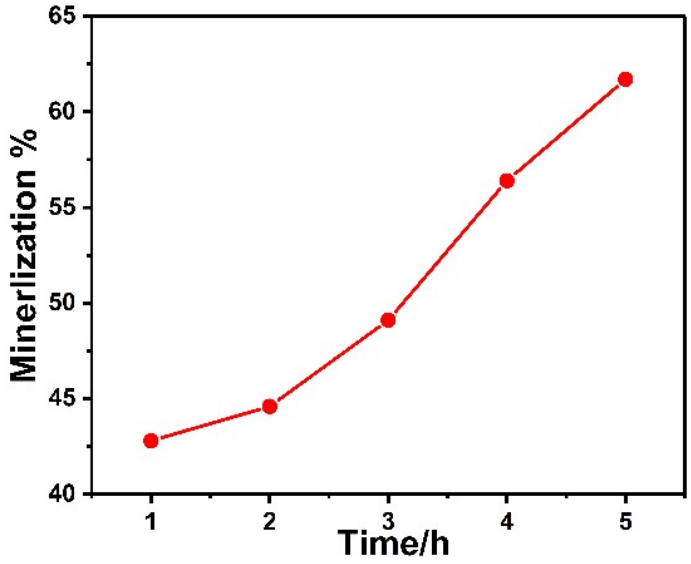

Fig. S7. TOC removal efficiency during the degradation of TCH using the AgBr@BiOBr/Bi_2O_3 photocatalyst.

S6. Comparison of the fresh and used catalysts

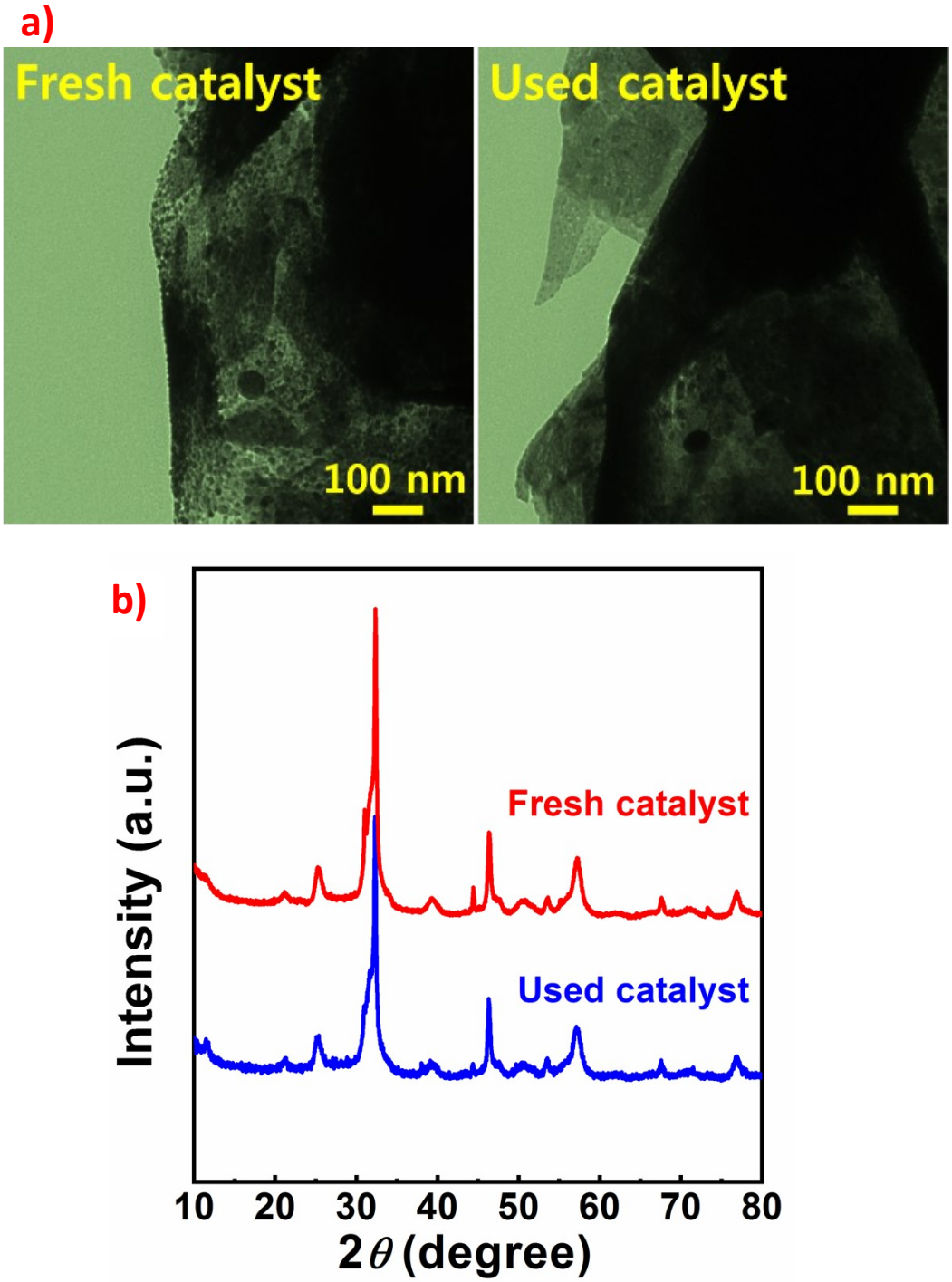

Fig. S8. TEM images (a) and XRD patterns (b) of Ag/AgBr@BiOBr/Bi_2O_3 catalysts (the fresh and the used for nine cycles).

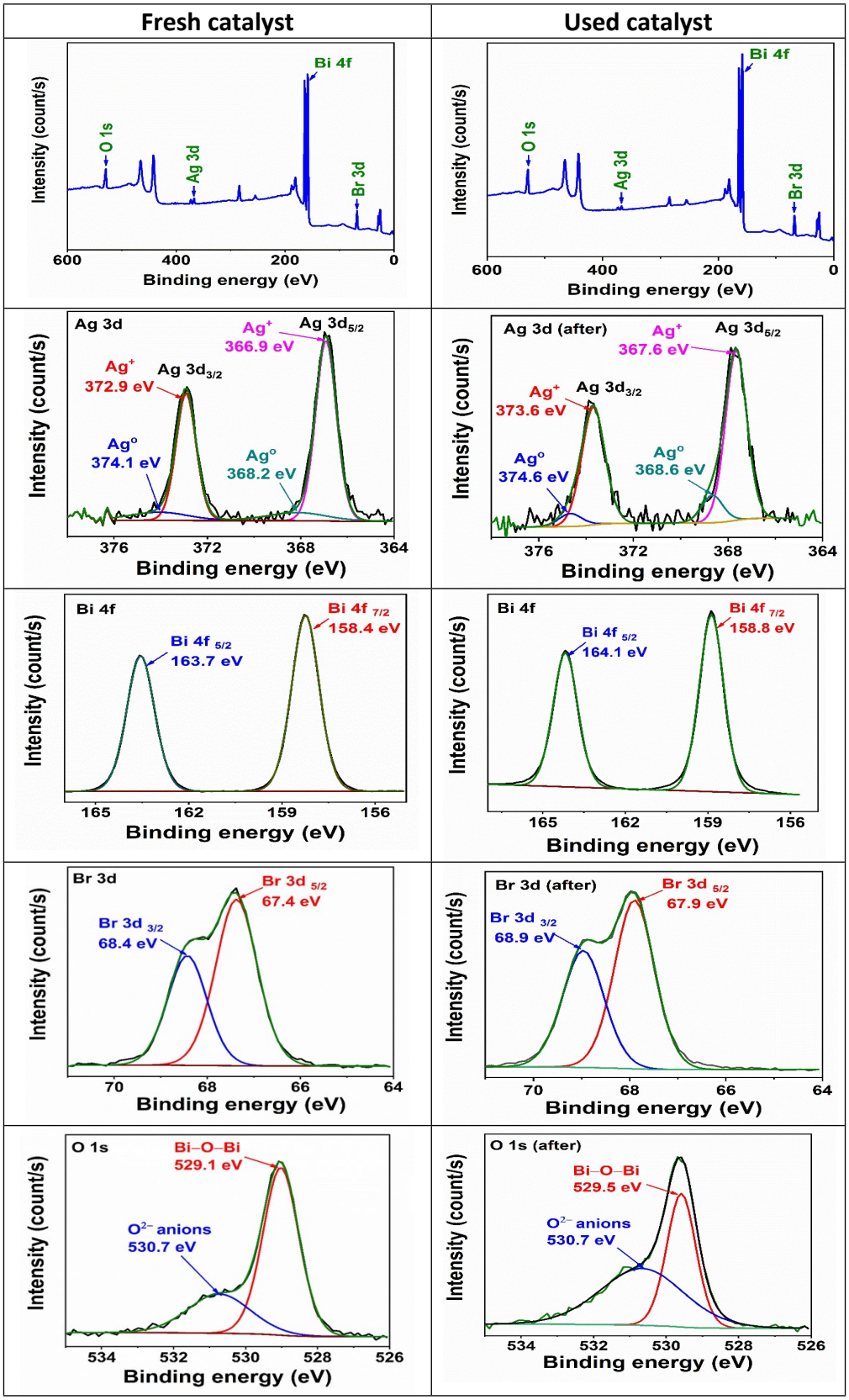
Fresh catalyst
Used catalyst
Intensity (count/s)
Binding energy (eV)
O 1s
Ag 3d
Bi 4f
Br 3d
Ag 3d
Ag+ 366.9 eV
Ag 3d5/2
Ag+ 372.9 eV
Ag 3d3/2
Ago 374.1 eV
Ago 368.2 eV
Ag 3d (after)
Ag+ 367.6 eV
Ag+ 373.6 eV
Ago 374.6 eV
Ago 368.6 eV
Bi 4f 7/2 158.4 eV
Bi 4f 5/2 163.7 eV
Bi 4f 7/2 158.8 eV
Bi 4f 5/2 164.1 eV
Br 3d 5/2 67.4 eV
Br 3d 3/2 68.4 eV
Br 3d (after)
Br 3d 5/2 67.9 eV
Br 3d 3/2 68.9 eV
O 1s
Bi–O–Bi 529.1 eV
O2− anions 530.7 eV
O 1s (after)
Bi–O–Bi 529.5 eV
O2− anions 530.7 eV

Fig. S9. XPS survey spectrum of the fresh and the 9-cycle-used Ag/AgBr@BiOBr/Bi_2O_3 catalyst.

S7. Tables of calculated data and comparison with literature

Table S1. Kinetic parameters (multiexponential fitted parameters and average lifetime) for emission decay of the as-prepared photocatalysts

Samples	A_1 (%)	τ_1 (ns)	A_2 (%)	τ_2 (ns)	A_3 (%)	τ_3 (ns)	A_4 (%)	τ_4 (ns)	$\boldsymbol{\tau_A}$ (ns)
AgBr	20.13	0.2646	0.65	2.70	79.22	0.0238	-	-	**0.69**
BiOBr/Bi_2O_3	12.07	4.6	0.12	120	87.81	0.723	-	-	**14.76**
Ag/AgBr@ BiOBr/Bi_2O_3	77.92	0.535	2.51	11	19.48	2.55	0.09	143	**16.75**

τ_i: Individual lifetime (ns)
A_i: the corresponding amplitude in a normalized percentage (%)
τ_A: Average lifetime of the charge carriers (ns).

Table S2. Photocatalytic activity of the Ag/AgBr@BiOBr/Bi_2O_3 catalyst (loading 0.3 g L^{-1}) in the degradation reaction of RhB (initial concentration 10 mg L^{-1}) for 60 min under visible light

Temperature (°C)	Apparent rate constant (k, min^{-1})	Degradation efficiency (η, %)	Regression coefficients R^2
25	0.073	91.4	0.99
35	0.116	95.0	0.99
45	0.146	99.3	0.97

Table S3. Performance of Ag- and Bi-containing photocatalysts in the literature and this study

Catalysts	Cat. load, w (g L^{-1})	Power of light source (W)	Degr. eff., η (%)	Pollu-tants	Initial conc., C_o (mg L^{-1})	Degr. time, t_d (min)	Perform. index, I	Ref.
BiOBr/BiOCl	1	500 W Xe lamp [λ > 390 nm]	86	RhB	10	90	19.1	[5]
α-Bi_2O_3/BiOBr	1	500 W Xe lamp [λ > 420 nm]	90	RhB	20	210	8.6	[6]
Ag QDs/BiOBr	0.2	300 W Xe lamp [λ > 400 nm]	97.9	RhB	20	20	815.8	[7]
AgBr/Bi_2O_3	1	500 W Xe lamp [λ > 400 nm]	92	RhB	5	60	30.7	[8]
BiOBr/Ag_3PO_4	0.5	500 W Xe lamp [λ > 420 nm]	99	RhB	5	30	132.0	[9]
Ag/β-Bi_2O_3	1	400 W X-W lamp [λ > 420 nm]	98	RhB	10	210	11.7	[10]
AgBr/{001} BiOCl	0.5	300 W Xe lamp [λ > 420 nm]	100	RhB	9.6	15	444.4	[11]
AgBr/{101} BiOCl	0.5	300 W Xe lamp [λ > 420 nm]	87.9	RhB	9.6	15	390.7	[11]
SnS_2/BiOBr	0.63	400 W Xe lamp [λ > 420 nm]	88	RhB	10	30	116.4	[3]
BiOBr/TiO_2	0.25	300 W Xe lamp [λ > 400 nm]	100	RhB	10	20	666.7	[12]
BiOBr/Bi_2O_3/ $BiO_{0.67}F_{1.66}$	0.5	500 W Xe lamp [λ > 420 nm]	98.6	RhB	10	15	262.9	[13]
AgBr/BiOBr	1	300 W Xe lamp [UV cut-off filter]	100	RhB	20	30	111.1	[14]
Ag/AgCl /BiOCl	0.8	500 W Xe lamp [λ > 400 nm]	100	RhB	10	50	50.0	[15]
Ag/AgBr@ BiOBr/Bi_2O_3	**0.3**	**2.4 W LED lamp [White light]**	**98**	**RhB**	**10**	**180**	**7561.7**	**This work**
"	**0.3**	**400 W Halogen lamp (OHP) [λ > 420 nm]**	**100**	**RhB**	**10**	**50**	**166.7**	**"**
Ag/AgI/ Bi_3O_4Cl	0.2	5 W- LED [White light]	61	MO	20	180	3389.0	[17]
Ag/Bi_2O_3	1	500 W Xe lamp [λ > 420 nm]	51	MO	20	180	5.7	[18]
AgBr/Bi_2O_3	1	500 W Xe lamp	92	MO	15	120	15.3	[19]

		[λ > 420 nm]						
AgBr/Ag/ BiOBr	2	300 W Xe lamp [-]	93	MO	26.7	40	38.7	[20]
Ag/AgBr@ $BiOBr/Bi_2O_3$	**0.3**	**400 W Halogen lamp (OHP) [λ > 420 nm]**	**96.6**	**MO**	**10**	**60**	**134.2**	**This work**
Ag/AgCl/BiOCl	0.4	500 W Xe lamp [λ > 400 nm]	81.2	TCH	10	120	33.8	[15]
Ag QDs/BiOBr	0.5	300 W Xe lamp [λ > 400 nm]	77.2	TCH	10	120	42.9	[7]
BiOBr/(CMC)	0.25	300 W Xe lamp [λ > 420 nm]	97	TCH	20	60	215.6	[16]
Ag/AgBr@ $BiOBr/Bi_2O_3$	**0.3**	**400 W Halogen lamp (OHP) [λ > 420 nm]**	**93.7**	**TCH**	**10**	**60**	**130.1**	**This work**
"	**0.5**	**150 W Xe lamp [λ =256–1900 nm]**	**98.6**	**TCH**	**10**	**60**	**219.1**	**"**

1. QD: quantum dot, CMC: carboxymethyl cellulose, OHP: overhead projector.
2. Performance index, $I = (\eta \times 10^4)/(w \times t_d \times P_l)$, η is the degradation efficiency (%), w is the catalyst loading (g L^{-1}), t_d is the degradation time (min), and P_l is the power of the lamp (W).

References

[1] B. Shao, Z. Liu, G. Zeng, Z. Wu, Y. Liu, M. Cheng, M. Chen, Y. Liu, W. Zhang, and H. Feng, Nitrogen-doped hollow mesoporous carbon spheres modified g-C_3N_4/Bi_2O_3 direct dual semiconductor photocatalytic system with enhanced antibiotics degradation under visible light, *ACS Sustainable Chem. Eng.* 2018, **6(12)**, 16424–16436.

[2] W. Li, Q. Chen, X. Lei, and S. Gong, Fabrication of Ag/AgBr/Ag_3VO_4 composites with high visible light photocatalytic performance, *RSC Adv.* 2019, **9(9)**, 5100–5109.

[3] F. Qiu, W. Li, F. Wang, H. Li, X. Liu, and J. Sun, *In-situ* synthesis of novel Z-scheme SnS_2/BiOBr photocatalysts with superior photocatalytic efficiency under visible light, *J. Colloid Interface Sci.* 2017, **493**, 1–9.

[4] H. Zhang, C.-G. Niu, S.-F.Yang, and G.-M. Zeng, Facile fabrication of $BiOIO_3$/BiOBr composites with enhanced visible light photocatalytic activity, *RSC Adv.* 2016, **6**, 64617.

[5] D. Ma, H. Liu, J. Huang, J. Zhong, J. Li, and D. Wang, Improved photocatalytic performance of flower-like BiOBr/BiOCl heterojunctions prepared by an ionic liquid assisted one-step hydrothermal method, *Mater. Lett*. 2019, **238**, 147–150.

[6] L. Shan, Y. Liu, H. Chen, Z. Wu, and Z. Han, An α-Bi_2O_3/BiOBr core–shell heterojunction with high photocatalytic activity, *Dalton Trans.* 2017, **46**, 2310.

[7] J. Di, J. Xia, M. Ji, B. Wang, S. Yin, Y. Huang, Z. Chen, and H. Li, New insight of Ag quantum dots with the improved molecular oxygen activation ability for photocatalytic applications, *Appl. Catal. B Environ.* 2016, **188**, 376–387.

[8] W. Gou, P. Wu, D. Jiang, and X. Ma, Synthesis of AgBr@Bi_2O_3 composite with enhanced photocatalytic performance under visible light, *J. Alloys Compd.* 2015, **646**, 437–445.

[9] J. Yan, M. Xu, B. Chai, and H. Wang, *In situ* construction of BiOBr/Ag_3PO_4 composites with enhanced visible light photocatalytic performances, *J. Mater. Res.* 2017, **32(8)**, 1603–1610.

[10] G. Zhu, W. Que, and J. Zhang, Synthesis and photocatalytic performance of Ag-loaded β-Bi_2O_3 microspheres under visible light irradiation, *J. Alloys Compd*. 2011, **509**, 9479–9486.

[11] Y. L. Qi, Y. F. Zheng, H. Y. Yin, and X. C. Song, Enhanced visible light photocatalytic activity of AgBr on {001} facets exposed to BiOCl, *J. Alloys Compd*. **2017**, 712, 535–542.

[12] X. X. Wei, H. Cui, S. Guo, L. Zhao, and W. Li, Hybrid BiOBr–TiO_2 nanocomposites with high visible light photocatalytic activity for water treatment, *J. Hazard. Mater.* 2013, **263**, 650–658.

[13] L. Cheng, J. Yan, S. Zhao, and L. Hao, Multiple charge carrier transfer pathways in $BiOBr/Bi_2O_3/BiO_{0.67}F_{1.66}$ ternary composite with high adsorption and photocatalytic performance, *J. Alloys Compd.* 2019, **778**, 924–932.

[14] L. Kong, Z. Jiang, H. L. Henry, J. N. Rebecca, T. Xiao, O. J. Martin, and P. E. Peter, Unusual reactivity of visible-light-responsive AgBr–BiOBr heterojunction photocatalysts, *J. Catal.* 2012, **293**, 116–125.

[15] S. Zhao, Y. Zhang, Y. Zhou, K. Qiu, C. Zhang, J. Fang, and X. Sheng, Reactable polyelectrolyte-assisted preparation of flower-like Ag/AgCl/BiOCl composite with enhanced photocatalytic activity, *J. Photochem. Photobiol. A: Chem.* 2018, **350**, 94–102.

[16] B. Xu, Y. Li, Y. Gao, S. Liu, D. Lv, S. Zhao, H. Gao, G. Yang, N. Li, and L. Ge, Ag-AgI/Bi_3O_4Cl for efficient visible light photocatalytic degradation of methyl orange: The surface plasmon resonance effect of Ag and mechanism insight, *Appl. Catal. B Environ.* 2019, **246**, 140–148.

[17] Y. Li, Z. Zhang, Y. Zhang, X. Sun, J. Zhang, C. Wang, Z. Peng, and H. Si, Preparation of Ag doped Bi_2O_3 nanosheets with highly enhanced visible light photocatalytic performances, *Ceram. Int.* 2014, **40**, 13275–13280.

[18] S. Yang, C. Chen, L. Liu, L. Zhu, and X. Xu, Facile fabrication of micro-floriated $AgBr/Bi_2O_3$ as highly efficient visible-light photocatalyst, *Mater. Res. Bull.* 2017, **92**, 29–38.

[19] Y. Dong, C. Feng, J. Zhang, P. Jiang, G. Wang, X. Wu, and H. Miao, A new p-metal-n structure AgBr-Ag-BiOBr with superior visible-light-responsive catalytic performance, *Chem. Asian J.* 2014. **00**, 0 – 0.

[20] M. Y. Liu, Y. F. Zheng, and X. C. Song, Biomass assisted synthesis of 3D hierarchical structure BiOX(X = Cl, Br)-(CMC) with enhanced photocatalytic activity, *J. Nanosci. Nanotechnol.* 2019, **19**, 5287–5294.